

METASOMATIC ORIGIN OF SPESSARTINE-RICH GARNET IN THE SOUTH MOUNTAIN BATHOLITH, NOVA SCOTIA

DANIEL J. KONTAK¹

Department of Earth Sciences, Memorial University, St. John's, Newfoundland A1B 3X5

MICHAEL COREY

Nova Scotia Department of Mines and Energy, 1496 Lower Water Street, Halifax, Nova Scotia B3J 2X1

ABSTRACT

An occurrence of spessartine-rich (15–25 mole %) almandine garnet within a late-stage, polyphase granitic intrusion (18–20 km²) of the 370-Ma-old South Mountain batholith, Nova Scotia, is described. Garnet occurs as euhedral to subhedral single grains or spherical quartz-garnet clots and is most abundant near contact zones, along fractures, and in late pegmatites. The garnet has an antipathetic relationship with biotite. Mineral chemistry of the major silicate phases of the host granitoids reflect re-equilibration with a fluid phase. For example, plagioclase compositions range from magmatic values (An₁₁₋₁₇) to those characteristic of a lower temperature metasomatic origin (An₀₋₅), biotite is anomalously enriched in Fe with Fe/(Fe + Mg) values of 0.85, and muscovite is characterized by lower wt. % Ti, Fe and Mg than is typical of magmatic muscovite. The petrographic and chemical data are interpreted to reflect a widespread interaction of hydrothermal fluids with the host granitoid that resulted in the post-magmatic growth of garnet. The development of the garnet, inferred to have occurred at temperatures in excess of 500°C based on two-feldspar geothermometry and textural relationships with sillimanite, cannot have occurred without contributions of Al, Fe, Mg and Mn from surrounding metasedimentary rocks. This occurrence of metasomatic garnet, of composition similar to that considered typical of magmatic garnets, again raises the problem of interpreting what is of primary magmatic origin in granitoid rocks.

Keywords: South Mountain batholith, peraluminous granite, metasomatism, garnet, Nova Scotia.

SOMMAIRE

Nous décrivons un exemple de grenat almandin à teneur importante en spessartine (15–25%, en fraction molaire) dans un granite polyphasé tardif (18–20 km²) du batholite de South Mountain (370 Ma), en Nouvelle-Écosse. Le grenat se trouve soit en cristaux uniques idiomorphes ou subidiomorphes, soit en amas sphériques avec du quartz, près des zones de contact, principalement, mais aussi le long de fissures, ou dans des pegmatites tardives. Le grenat définit une relation d'incompatibilité avec la biotite. La com-

position chimique des silicates principaux du granite est régie par un épisode de ré-équilibre avec une phase fluide. À titre d'exemples, la composition du plagioclase varie entre la composition magmatique (An₁₁₋₁₇) et celle caractéristique d'un métasomatisme de basse température (An₀₋₅); la biotite est anormalement enrichie en fer, et le rapport Fe/(Fe + Mg) atteint 0.85; enfin, la muscovite est appauvrie en Ti, Fe et Mg comparée à une muscovite magmatique typique. Les données pétrographiques et chimiques indiqueraient une interaction répandue du granite avec une phase fluide introduisant les éléments Al, Fe, Mg et Mn, qui sont lessivés des roches métasédimentaires encaissantes. C'est ce fluide qui est responsable de la croissance post-magmatique du grenat à une température supérieure à 500°C, laquelle est définie par la coexistence des deux feldspaths et les relations texturales avec la sillimanite. Cet exemple de grenat métasomatique, qui possède une composition considérée comme typique de celle d'un grenat magmatique, illustre bien le problème de trouver les composants d'origine primaire dans une roche granitique.

(Traduit par la Rédaction)

Mots-clés: batholite de South Mountain, granite hyperalumineux, métasomatisme, grenat, Nouvelle-Écosse.

INTRODUCTION

Garnet in felsic igneous rocks can have multifarious origins (e.g., Pattison *et al.* 1982, Miller & Stoddard 1981, Allan & Clarke 1981, Hamer & Moyes 1982), which have been reviewed by Clarke (1981), who suggested (p. 10) that only "...a very thorough textural and chemical investigation will permit clear discrimination among these competing models". Most authors have discussed the origin of garnet in felsic igneous rocks under two general subdivisions, either xenocrystic or phenocrystic/magmatic, although a metamorphic origin has been alluded to for some occurrences in metavolcanic rocks (e.g., Ryan 1984).

The purpose of this communication is to describe an occurrence of spessartine-rich almandine garnet occurring in the South Mountain batholith (SMB) of Nova Scotia, for which a metasomatic origin is suggested. Although Allan & Clarke (1981) recently discussed the occurrence and origin of three types

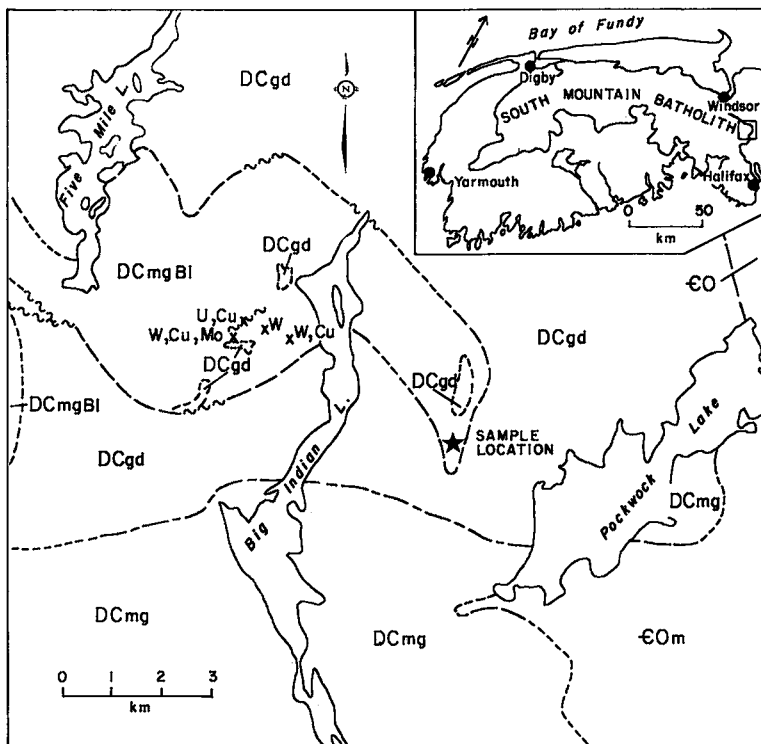
¹ Present address: Nova Scotia Department of Mines & Energy, 1496 Lower Water Street, Halifax, Nova Scotia B3J 2X1

of garnet in the SMB, the type to be described herein was not mentioned.

The SMB is a post-tectonic, peraluminous granodiorite-monzogranite-leucocratic monzogranite complex of 10,000 km² outcropping in the Meguma Zone of the Appalachian Orogen (McKenzie & Clarke 1975). The batholith has been dated by the Rb-Sr technique at 372-361 Ma (Clarke & Haldiday 1980) and Reynolds *et al.* (1981) have reported an average age of 366 ± 4 Ma based on 23 K-Ar and Ar-Ar dates. The general petrological features are discussed by McKenzie & Clarke (1975), and more recently Clarke & Muecke (1985) and Clarke & Chatterjee (1985) who have presented comprehensive

accounts of the geological, geophysical and isotopic features of the SMB.

The study area is 30 km northwest of Halifax, between Pockwock and Big Indian Lakes (Fig. 1) in an area previously shown to be underlain predominantly by biotite granodiorite (Keppie 1979). However, recent mapping of this terrane (Corey 1986) has shown that the area consists of a granodiorite-monzogranite complex [IUGS classification of Streckeisen (1976) used throughout] with lesser amounts of late-stage microgranite plugs, dykes and pegmatites. This complex, referred to as the Big Indian Polyphase Intrusive (BIP) body, was infiltrated by late-stage fluids that promoted the



LEGEND

- EOm undivided metasediments of the Meguma Group
- DCgd biotite granodiorite
- DCmg biotite ± muscovite ± cordierite monzogranite
- DCmgBI undivided rocks of the Big Indian Polyphase Intrusion (see Table 1)

x^W.....mineral occurrence

FIG. 1. Location and generalized geological map of the study area. Location of samples examined in this study are indicated.

development of numerous secondary minerals, including the peraluminous mineral assemblage muscovite, garnet, andalusite and sillimanite (Corey 1987). This locality represents the first reported occurrence of sillimanite in the SMB, the details of which will be discussed elsewhere (M. Corey, in prep.).

GEOLOGICAL SETTING

The BIPI complex, located near the northern margin of the SMB (Fig. 1), intruded an earlier granodiorite phase of the batholith, itself bounded to the north and east by metasedimentary rocks of the Cambro-Ordovician Meguma Group. The granodiorite is medium- to coarse-grained, K-feldspar megacrystic and biotite-rich, and is characterized by the presence of abundant metasedimentary xenoliths (Meguma Group lithologies) that are variable in size (< 5 cm to > 20 m) and degree of assimilation. Occurring south of the BIPI complex is a medium- to coarse-grained, variably K-feldspar megacrystic, biotite-muscovite \pm cordierite monzogranite unit currently referred to as the Sandy Lake monzogranite. Although indicated as a single unit in Figure 1, it consists of several phases.

The BIPI complex (Fig. 1, Table 1) consists of strongly peraluminous, biotite-muscovite-garnet \pm cordierite granitoid rocks (Fig. 2) outcropping over an areal extent of 18–20 km². Significant amounts of polymetallic W-Cu \pm Mo and U-Cu vein mineralization is present where local zones of intense shearing and hydrothermal alteration occur. Numerous roof pendants of the granodiorite occur in the BIPI complex, but metasedimentary xenoliths are notably lacking.

The BIPI complex has been tentatively divided into four phases that are mineralogically similar, but texturally variable (Table 1). These subdivisions include, in decreasing order of abundance: (i) coarse-grained, equigranular to seriate, slightly K-feldspar megacrystic, two-mica monzogranite, (ii) fine- to medium-grained, equigranular, two-mica monzogranite to leucocratic (< 5% biotite) monzogranite, (iii) very fine-grained, saccharoidal monzogranite-syenogranite (herein referred to as a microgranite), and (iv) quartz-feldspar porphyry. These phases display intimate spatial relationships and sharp, irregular contacts. Field relationships indicate that the coarse-grained monzogranite represents the earliest intrusive phase, but the temporal relationships of the other units remain unresolved. Pegmatitic segregations and aplitic dykes are found associated with all the phases, indicating that locally the melts were water-saturated.

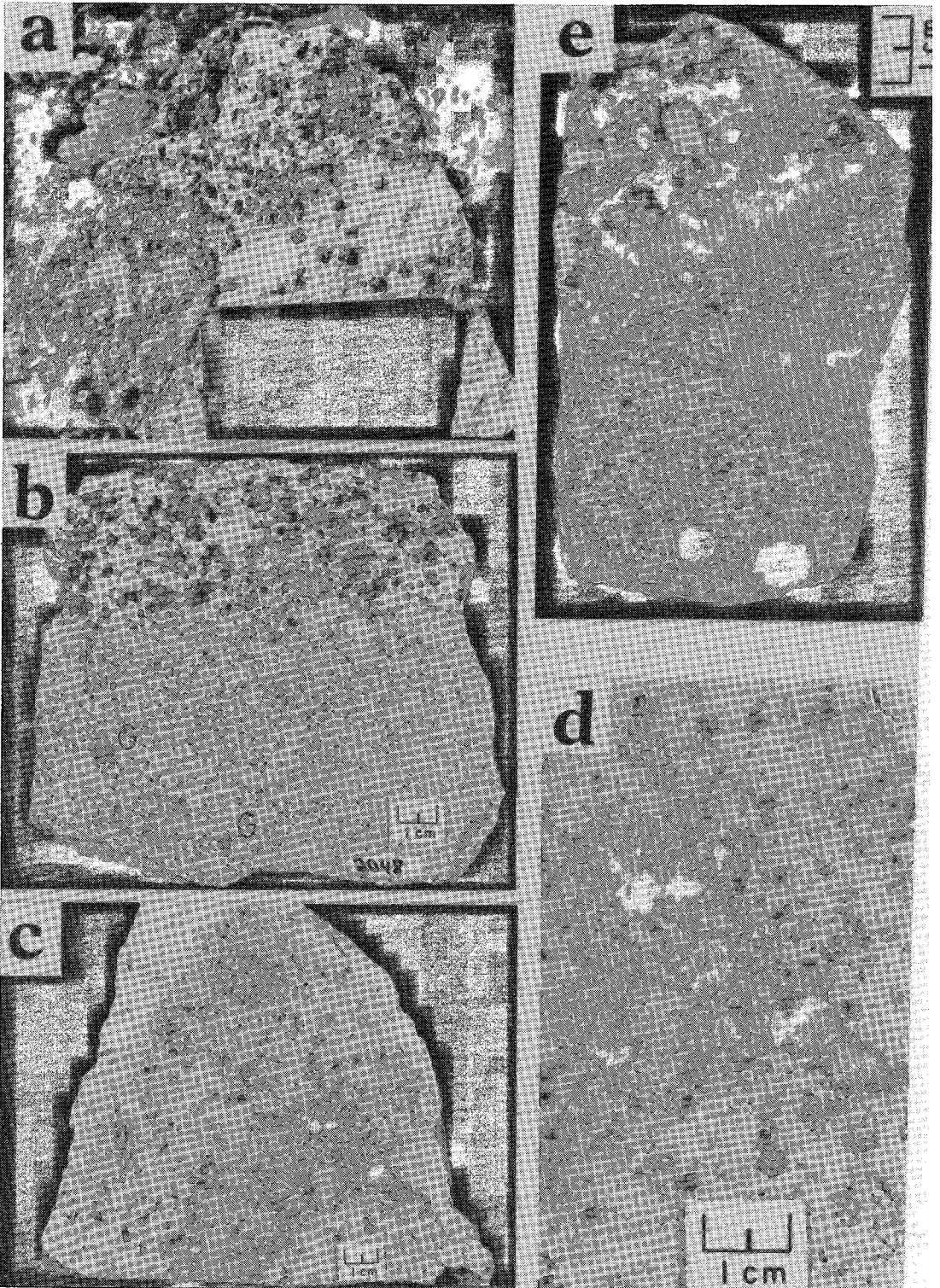
The mineralogy of the different magmatic units is similar (Table 1), consisting predominantly of quartz, K-feldspar and plagioclase + biotite + garnet + cordierite + muscovite. Garnet (Figs. 2, 3) occurs most commonly as 0.1 to 1 cm, rounded to subrounded, reddish crystal aggregates. Euhedral grains, 0.1 to 0.5 cm across, are less common. Although the garnet grains are disseminated throughout the rocks, they also occur concentrated along fractures (Figs. 2c, d) which have selvages enriched in alkali feldspar. Garnet also occurs as an accessory phase in quartz-orthoclase-albite-muscovite-tourmaline pegmatites which cut the monzogranite. The presence of garnet is the most reliable field criterion for distinguishing rocks of the BIPI complex from the other intrusive phases in the region.

The BIPI complex exhibits various types of alteration (e.g., albitization, hematitization, chloritiza-

TABLE 1. PETROGRAPHIC DESCRIPTION OF THE BIG INDIAN POLYPHASE INTRUSION

Unit	Description						
	General			Mineralogy (Visual Modal Estimates)			
Big Indian Lake Polyphase Intrusion	Colour	Grain Size	Texture	Bt	Ms	Crd	Kfs Megacryst
coarse grained monzogranite	medium grey buff	coarse with some phenocrysts	seriate hypidiomorphic granular	4 - 8%	trace - 3%	trace - 2%	<2%
fine- to medium-grained monzogranite	buff to orange, brown	fine to medium	equigranular - seriate	3 - 6%	1 - 4%	trace - 1%	absent
microgranite	buff to white	very fine grained	saccharoidal	<5%	trace - 1%	1%	absent
porphyry	buff to light grey	fine to medium with coarse grained phenocrysts	porphritic	3 - 10%	trace - 1%	absent	absent

Abbreviations: Bt = biotite; Ms = muscovite; Crd = cordierite; Kfs = K-feldspar
Mineralogy described represents primary magmatic phase only



tion, biotitization, tourmalinization, silicification and greisenization), but the alteration is confined to the central part of the BIPI complex where mineralization occurs (Fig. 1). The alteration is most intense within late shear zones where the primary mineralogy of the granites has been modified to the assemblage andalusite, sillimanite, cordierite, garnet, muscovite, biotite and tourmaline. Textural relationships indicate a complex hydrothermal origin for these minerals that involved several generations of superimposed alteration events (Corey 1987). From a paragenetic viewpoint, the garnet predates all of the alteration stages.

PETROGRAPHY OF THE ANALYZED SAMPLES

Three garnet-bearing samples from the southeastern part of the BIPI complex (Fig. 1) were selected for detailed analysis of the major silicate minerals: (1) muscovite-biotite monzogranite (NS-46-2), (2) muscovite leucogranite dyke (NS-46-1) that cuts the aforementioned monzogranite, and (3) muscovite-biotite microgranite (NS-48-1,2,3). The first two samples are from the same large outcrop, whereas the third was collected a few hundred meters from it. All of the phases are garnet-bearing.

(1) The *biotite-muscovite-garnet monzogranite* (1 in Table 1) is medium- to coarse-grained, hypidiomorphic granular. Quartz occurs as subhedral grains and displays variably developed undulatory extinction. Plagioclase (average An_{20} , weakly zoned) is euhedral to subhedral; where saussuritized the alteration is concentrically zoned about the core of the feldspar. Abundant coarse secondary muscovite \pm chlorite clots replaced some plagioclase cores. K-feldspar (monoclinic variety as determined from XRD study) occurs as subhedral to euhedral megacrysts up to a few cm long and is slightly perthitic. Biotite is subhedral to euhedral, has an orange-brown color where freshest, and contains variable amounts of zircon and apatite. Adjacent to the dyke, biotite is variably chloritized, or is absent, but a few chlorite grains attest to its earlier presence. Muscovite occurs in a variety of textures, the most common being isolated grains or aggregates of subhedral to rarely euhedral habit that appear to overgrow adjacent quartz and feldspar (Figs. 4a, c). Less commonly, muscovite occurs as rosettes between other

silicates or within them (*e.g.*, plagioclase: Fig. 4b), and also as a mantle surrounding garnet. Garnet (1–7 mm), of red to orange-red color, occurs as euhedral grains that are dominantly inclusion-free and clearly cross-cut the other minerals, indicating a late-stage growth. Although randomly distributed throughout the rock, the garnet is notably enriched (up to 40%) where the monzogranite is cut by either leucogranite dykes (Fig. 2e) or microgranite (Figs. 2a, b). Inclusions (< 1–2%) include muscovite occurring along fractures, and titanite and epidote, both of which occur as single, euhedral to subhedral grains or aggregates.

(2) The *muscovite-garnet leucocratic dyke* is fine-grained (av. grain size < 1 mm), hypidiomorphic, equigranular, and contains up to several percent garnet (Figs. 2e, 3j). The rock shows abundant textural evidence of re-equilibration, including recrystallization of minerals (*e.g.*, quartz), abundant fluid-inclusion trails in quartz, and development of seriate or sacchroidal to allotriomorphic texture. Quartz is subhedral to euhedral, free of mineral inclusions, and occurs either as a separate phase or intergrown with garnet (Figs. 3g, h, i). In the latter case quartz is similar in texture and grain size to those grains that surround garnet. Plagioclase, invariably albitic, occurs as euhedral to subhedral grains either as a discrete, isolated phase, or as replacements of K-feldspar. In these replacements, much of the plagioclase displays chessboard-type texture, a feature commonly observed in alkali-metasomatized granites (*e.g.*, Martin & Bowden 1981). K-feldspar, dominantly the orthoclase variety, is subhedral to anhedral and contains variable amounts of exsolved albite. Inversion to a triclinic phase is only on a very minor scale, with individual grains showing development of discrete domains of grid-twinned microcline with the bulk of the grain characterized by a mottled birefringence indicative of intermediate microcline (*cf.* Fig. 4b of Černý *et al.* 1984). Muscovite, generally < 1–2 vol.% and inclusion free, occurs as subhedral to ragged, anhedral grains of variable grain size (< 5 mm), which may be isolated or show an obvious replacement texture. Garnet occurs as subrounded clots 1 to > 10 mm across and is invariably intergrown with anhedral quartz (Figs. 3g, h, i). The garnet grains that form the marginal portions to these clusters have an idiomorphic outline (Fig. 3g). All the garnet grains are inclusion-

FIG. 2. Specimens of garnetiferous granites in the BIPI complex: (2a) Two-mica garnet monzogranite phase (top of photo) in contact with the microgranite. Note the concentration of garnet at the contact (scale is in cm); (2b) a slabbed section illustrating the contact shown in (2a). The garnet grains (G) in the microgranite are characterized by their subhedral outlines and quartz inclusions; (2c) sample of the microgranite containing garnet grains aligned along a fracture extending the length of the sample (lower right to upper left); (2d) enlargement of the garnet-bearing part of (2c) showing the subhedral forms of the garnet and symplectic textures; (2e) contact between monzogranite and leucocratic dyke-rock. Note the concentration of garnet at the contact (small, dark, euhedral grains), and coarse, subhedral garnet with symplectic textures in the bottom of the photograph.

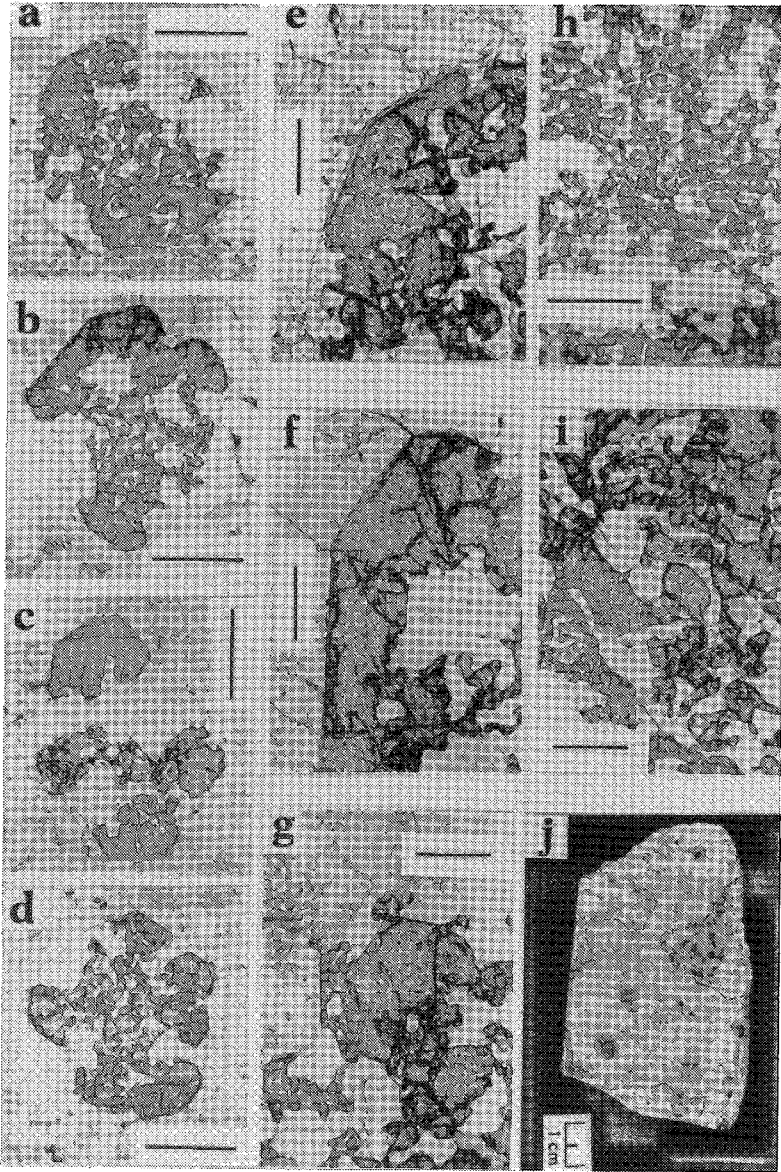


FIG. 3. Plane-polarized light photomicrographs (except for rock photo in 3j) of garnet in granites of the BIP1 complex. (3a,b,c,d): garnet-quartz intergrowths in the microgranite. The garnet grains generally have pseudo-euhedral to subhedral outlines, are intergrown only with quartz, and are mantled with narrow selvages of muscovite (scale bar = 1.5 mm in all photos). (3e) Enlargement of the garnet in Figure 3a showing the muscovite mantle (scale bar 0.5 mm). (3f) Enlargement of the garnet in Figure 3b, showing the muscovite mantle and euhedral habit of the garnet (scale bar 0.5 mm). (3g,h,i) Garnet clots, in the leucocratic dyke-rock, consisting of clusters of anhedral garnet intergrown with quartz. The garnet attains good crystal forms only at the margins of the clots (e.g., Fig. 3g; scale bar 1.5 mm in g and h and 0.5 mm in i). (3j) Sample of the microgranite showing the inverse modal relationship between garnet (found in the leucocratic part of the rock only) and biotite (area outlined by dashed line).

free, the only exception being trace amounts of chlorite, chloritized biotite, and euhedral to subhedral titanite. Marginal to the monzogranite, small (2 mm) euhedral grains of garnet occur (Fig. 2e), similar in texture to those found in the monzogranite itself.

(3) The *biotite-muscovite-garnet microgranite* (3 in Table 1) is fine-grained, hypidiomorphic to xenomorphic, equigranular. Quartz, of subhedral to anhedral habit, is generally inclusion-free except where it occurs intergrown with or adjacent to garnet, in which case it may contain rutile needles. Plagioclase, of albitic composition, is finely twinned,

euhedral to subhedral, slightly zoned, inclusion-free, and rarely shows undulatory extinction and bent twin lamellae. K-feldspar, of subhedral to anhedral habit, is generally perthitic (film, string, vein varieties) and although grid-twinned microcline is locally developed, orthoclase and intermediate microcline are most common. Biotite is present as ragged, subhedral to anhedral, medium to light brown and brownish green grains; the color variation reflects different degrees of chloritization or replacement by muscovite. The freshest biotite occurs in areas not containing garnet, and the two minerals display a strong



FIG. 4. Photomicrographs of muscovite grains in granitoid rocks of the BIPI complex. Note the generally subhedral habit, but ragged margins, as outlined in black. (4a) Muscovite surrounded by altered plagioclase grains in the monzogranite (plane-polarized light; scale bar 1.5 mm). (4b) Muscovite rosettes replaced the core of a saussuritized plagioclase grain in the monzogranite (crossed Nicols; scale bar 1.5 mm). (4c) Muscovite grain of secondary origin in monzogranite (crossed Nicols; scale bar 1.5 mm). (4d) Muscovite replacement of biotite in the microgranite (plane-polarized light; scale bar 0.5 mm).

(0.5–1 mm) to medium (5–6 mm), subhedral to anhedral, pale to dark red grains in bleached parts of the granite (*i.e.*, areas in which biotite is scarce to absent: see Fig. 3j). The garnet (Figs. 3a,b,c,d) contains variable amounts (0–30 vol.%) of quartz intergrowths, but is itself inclusion-free. In this way the garnet resembles that found in the dyke-rock previously described. Other mineral phases include minor chlorite, zircon, andalusite and sillimanite. The sillimanite and andalusite display complex textural relationships with biotite, which they replaced, and muscovite.

In summarizing, the salient aspects of the petrographic features of the three garnet-bearing samples are: (i) the pervasive development of albite, (ii) the highly variable textural and structural states of the alkali feldspars, (iii) the late-stage overgrowths of muscovite which replaced garnet, feldspars and biotite, (iv) the highly irregular morphology of garnet which occurs as euhedral grains in the monzogranite and margins of the dyke-rock, but as anhedral clusters with quartz intergrowths elsewhere. Textures indicate that garnet developed late: it overgrew most of the silicate phases, and (v) garnet and biotite show an antipathetic relationship.

MINERAL CHEMISTRY

Mineral compositions (plagioclase, K-feldspar, biotite, muscovite, garnet) were measured using a three-spectrometer JEOL JXA-50A automated electron microprobe with Krisel programming; natural silicate minerals were used as standards. Normal operating conditions were as follows: accelerating voltage 15 kV, sample current 0.02 μ A, and a beam

TABLE 3. REPRESENTATIVE COMPOSITIONS OF ALKALI FELDSPAR

ANALYSIS NUMBER	149	150	134	135	13	12
SiO ₂	65.88	66.08	65.81	66.27	64.64	63.96
Al ₂ O ₃	18.51	18.34	18.68	18.79	18.83	18.70
Na ₂ O	0.94	0.79	1.19	1.33	1.10	1.41
K ₂ O	14.77	14.75	14.79	14.21	14.83	14.52
Total	100.10	99.96	100.47	100.60	99.40	98.59
NUMBER OF CATIONS ON THE BASIS OF 8 OXYGEN						
Si	3.011	3.025	3.003	3.009	2.987	3.037
Al	0.997	0.988	1.004	1.005	1.026	1.047
Na	0.083	0.068	0.104	0.117	0.099	0.130
K	0.861	0.861	0.861	0.823	0.874	0.880
END MEMBER FELDSPARS IN MOLECULAR PER CENT						
Ab	8.8	7.3	10.8	12.4	10.1	12.9
An	0.0	0.0	0.0	0.0	0.0	0.0
Or	91.2	92.7	89.2	87.6	89.9	87.1

Analyses are from the following samples
 NS-46-1 : 149,150 NS-48-3 : 12,13
 NS-48-2 : 134,135

diameter of 2 μ m (15 μ m for feldspar analysis). The data were corrected on-line by the Bence & Albee (1968) method, and the precision and accuracy were monitored by analyzing well-characterized standards.

Plagioclase compositions (representative values given in Table 2; data plotted in Fig. 5) vary from An₁₁₋₁₇ in the monzogranite to An₀₋₅ in the dyke-rock and microgranite, with a small amount of zoning present.

Compositions of K-feldspars coexisting with plagioclase (Table 3) were determined for the dyke-rock and microgranite and range from Or₈₂ to Or₉₅ (Fig. 5). The broad spectrum in compositions presumably reflects the variable extents of re-equilibration and exsolution that occurred during subsolidus cooling. No data were obtained for the

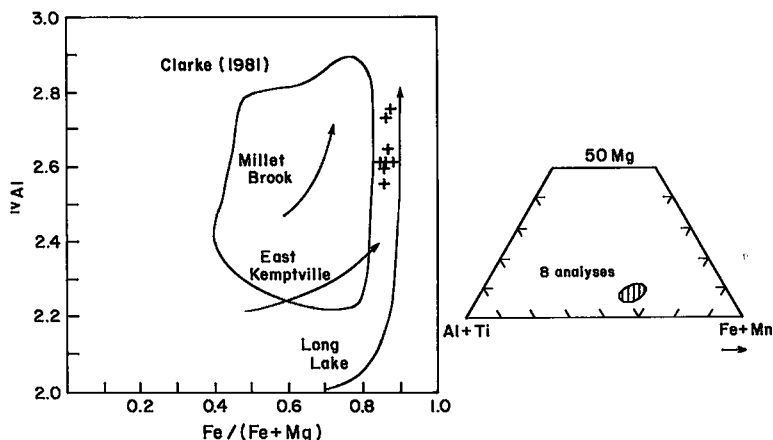


FIG. 6. Analyses of biotite from the microgranite of the BIP1 complex plotted in: (i) the ¹⁴Al versus Fe/(Fe+Mg) diagram, with Clarke's (1981) field for biotites in peraluminous granites, and data for biotite from different localities in the SMB (Chatterjee & Strong 1985); and (ii) Foster's (1960) trioctahedral diagram.

TABLE 4. COMPOSITIONS OF BIOTITE IN SAMPLE NS-48-3

ANALYSES NUMBER	COMPOSITIONS OF BIOTITE IN SAMPLE NS-48-3								
	18	19	32	35	36	138	139	140	
SiO ₂	33.62	33.48	33.89	34.09	33.62	34.02	32.72	33.67	
TiO ₂	1.38	1.38	1.45	1.31	1.27	1.75	1.48	1.39	
Al ₂ O ₃	20.38	20.09	19.69	20.23	20.44	20.58	21.09	22.12	
FeO	27.79	28.55	27.42	28.02	27.36	27.38	27.59	27.21	
MnO	0.46	0.32	0.42	0.31	0.24	0.27	0.30	0.32	
MgO	2.31	2.24	2.65	2.64	2.70	2.30	2.40	2.36	
CaO	ND	0.02	ND	ND	ND	ND	ND	0.02	
K ₂ O	8.07	8.70	8.44	8.54	7.96	8.42	8.54	8.67	
Cr ₂ O ₃	0.02	ND	ND	ND	ND	0.02	0.01	ND	
Na ₂ O	0.07	0.12	0.03	0.04	0.07	0.02	0.06	0.10	
Total	94.30	94.91	94.01	95.18	93.65	94.79	94.16	95.85	
NUMBER OF CATIONS ON THE BASIS OF 11 OXYGENS									
Si	2.695	2.674	2.713	2.698	2.689	2.691	2.618	2.629	
Al ^{iv}	1.305	1.326	1.288	1.302	1.311	1.309	1.382	1.371	
Al ^{vi}	0.608	0.560	0.570	0.584	0.616	0.609	0.607	0.665	
Ti	0.082	0.083	0.087	0.078	0.076	0.086	0.086	0.080	
Fe ²⁺	1.852	1.907	1.838	1.853	1.830	1.811	1.846	1.776	
Cr	0.001	0.000	0.000	0.000	0.000	0.000	0.000	0.000	
Mn	0.031	0.022	0.028	0.021	0.017	0.016	0.019	0.029	
Mg	0.274	0.266	0.316	0.311	0.322	0.284	0.284	0.272	
K	0.820	0.886	0.862	0.862	0.812	0.850	0.871	0.864	
Na	0.022	0.018	0.004	0.003	0.011	0.002	0.007	0.014	
Ca	0.000	0.001	0.000	0.000	0.000	0.000	0.000	0.000	
Fe/(Fe+Mg)	0.871	0.867	0.853	0.856	0.850	0.864	0.867	0.867	

ND = not detected

monzogranite at this particular locality, but bulk compositions of K-feldspar separates from other monzogranites of the SMB have a narrow range, from Or₆₀ to Or₆₈ (Kontak, unpubl. data).

The compositions of coexisting feldspars are sensitive to temperature and thus have the potential to be used as a geothermometer, although there are inherent problems with the method (Parsons & Brown 1984). However, we note that there are major differences between the temperatures obtained for

the different rock types when the data are plotted on the two-feldspar geothermometer diagram (Fig. 5) irrespective of the structural state of the alkali feldspar used in the calibration. The feldspars in the monzogranite have retained compositions which approach magmatic conditions (*i.e.*, 600–650°C to 800°C, depending on the model curve), although the presence of albitic plagioclase (An₂₋₆), as indicated from some of the analyses in this sample (Fig. 5), reflects some later re-equilibration at lower temperatures. In contrast, the feldspar data for the dyke-rock and microgranite (shown together in Fig. 5) record much lower temperatures (*ca.* 350 to 500°C, both for sanidine and microcline curves). These lower temperatures are consistent with petrographic observations in which muscovite replaced andalusite, and microcline occurs at the expense of orthoclase.

Biotite compositions (Table 4) were obtained only for one sample of the microgranite phase (sample NS-48-3). These pale orange-brown grains are predominantly annite–siderophyllite, with a narrow range in Fe/(Fe + Mg) values (0.850 to 0.871), ^{iv}Al contents between 1.288 to 1.382 (based on 11 oxygen atoms per formula unit), and low absolute abundances of Ti (1.4 wt. % TiO₂), Mg (2.5 wt. % MgO) and Mn (0.3–0.4 wt. % MnO). The biotite is slightly more Fe-rich than the field outlined by Clarke (1981; Fig. 6) for biotite in peraluminous rocks, and corresponds to the Fe-rich region in Foster's (1960) tri-

TABLE 5. REPRESENTATIVE COMPOSITIONS OF MUSCOVITE

ANALYSES NUMBER	REPRESENTATIVE COMPOSITIONS OF MUSCOVITE									
	45	56	126	84	87	142	143	8	15	21
SiO ₂	47.15	45.84	47.42	46.78	47.39	48.30	47.02	46.52	45.98	46.25
TiO ₂	0.23	0.50	0.41	0.30	0.28	0.12	0.16	0.00	0.00	0.09
Al ₂ O ₃	35.59	36.15	35.36	37.54	35.21	36.32	36.04	37.37	36.41	36.49
FeO	1.67	1.37	1.98	1.45	1.55	1.63	1.88	1.25	1.82	1.39
MnO	0.03	0.00	0.01	0.01	0.09	0.03	0.03	0.01	0.03	0.04
MgO	0.25	0.50	0.77	0.51	0.72	0.46	0.31	0.11	0.38	0.23
K ₂ O	9.78	9.11	9.97	9.50	9.66	9.52	9.61	8.84	9.31	9.57
Na ₂ O	0.17	0.70	0.33	0.43	0.35	0.53	0.43	0.27	0.43	0.39
Cr ₂ O ₃	ND	0.01	0.01	ND	ND	0.03	0.04	ND	0.04	0.02
Total	94.88	94.18	96.26	96.52	95.27	96.95	95.51	94.33	94.40	94.47
NUMBER OF CATIONS ON THE BASIS OF 11 OXYGEN										
Si	3.128	3.060	3.115	3.047	3.131	3.131	3.104	3.078	3.068	3.079
Al ^{iv}	0.871	0.940	0.885	0.953	0.869	0.869	0.896	0.922	0.932	0.920
Al ^{vi}	1.912	1.906	1.852	1.930	1.673	1.904	1.908	1.993	1.932	1.944
Ti	0.011	0.025	0.019	0.013	0.013	0.005	0.007	0.000	0.000	0.004
Fe ²⁺	0.092	0.076	0.108	0.078	0.085	0.087	0.103	0.069	0.102	0.078
Mg	0.024	0.050	0.075	0.047	0.069	0.043	0.029	0.011	0.038	0.023
Mn	0.001	0.000	0.000	0.000	0.003	0.000	0.000	0.001	0.002	0.002
Cr	0.000	0.000	0.000	0.000	0.000	0.000	0.000	0.000	0.002	0.001
K	0.828	0.776	0.834	0.788	0.814	0.786	0.808	0.746	0.792	0.813
Na	0.022	0.090	0.040	0.053	0.044	0.066	0.054	0.035	0.056	0.050
Ca	0.000	0.000	0.000	0.000	0.000	0.000	0.000	0.000	0.000	0.000

Analyses are from the following samples:

NS-46-1 : 84,87 NS-48-2 : 142,143
 NS-46-2 : 45,56,126 NS-48-3 : 8,15,21

Muscovite analyses represent the following textural types: rimming garnet (45,8); replacing biotite (21,142); replacing K-feldspar (143); isolated secondary grains (56,126,84,87,15)

ND = not detected

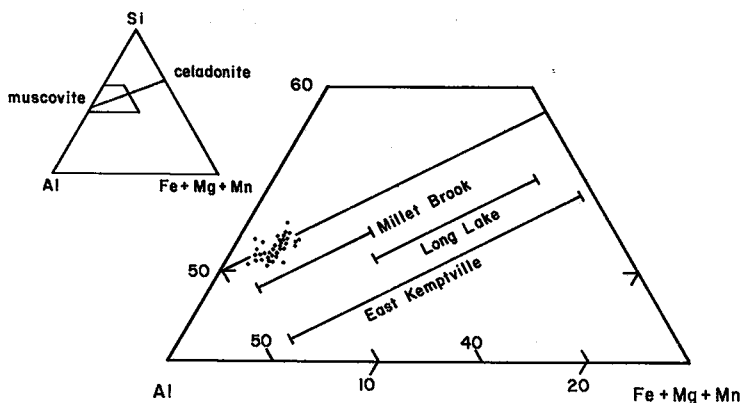


Fig. 7. Compositions of muscovite in the BIPI complex plotted in the ternary diagram Al-Si-(Fe + Mn + Mg). Note that the data from Millet Brook, Long Lake and East Kempville (from Chatterjee & Strong 1985) also fall on or about the muscovite-celadonite join.

octahedral plot (Fig. 6). Compared with biotite data obtained for various phases of the SMB (Allan & Clarke 1981, Chatterjee & Strong 1985, Chatterjee *et al.* 1985) and adjacent Musquodoboit batholith (MB) (MacDonald 1982), the biotite in NS-48-3 is generally more evolved (*i.e.*, Fe-rich).

The white micas approach end-member muscovite

in composition (Table 5) with Fe (0.9 to 1.9 wt.% FeO) the most abundant "impurity", expressed as a celadonitic component (Fig. 7). Additional constituents include minor amounts of Na (0.16 to 0.68 wt.% Na₂O) and Mg (0.18 to 0.7 wt.% MgO), and traces of Ti, Cr and Ca. Although several different textural varieties of muscovite are recognized, no

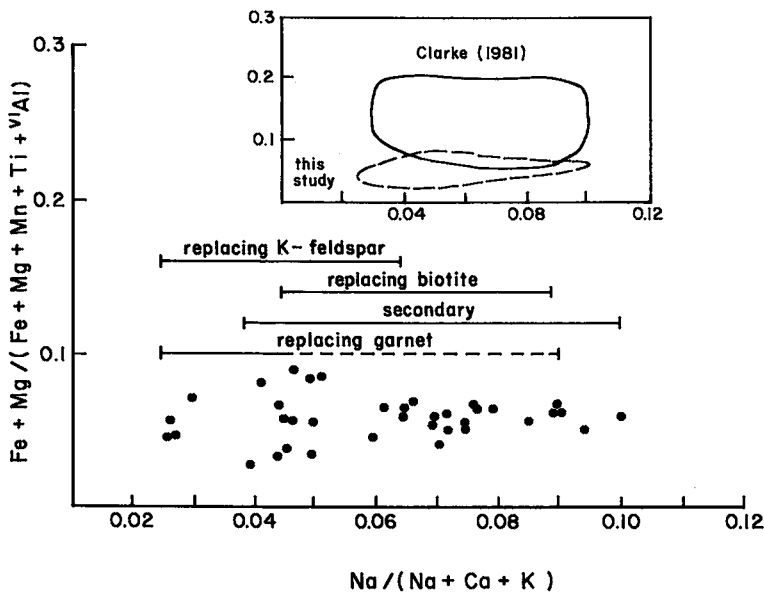


Fig. 8. Compositions of muscovite in the BIPI complex plotted in the $\text{Na}/(\text{Na} + \text{Ca} + \text{K})$ versus $(\text{Fe} + \text{Mg})/(\text{Fe} + \text{Mg} + \text{Mn} + \text{Ti} + {}^{\text{v}}\text{Al})$ diagram showing the compositional ranges (indicated by the lines) for the different textural varieties of muscovite. The results of this study are compared to muscovite compositions from peraluminous granitoid rocks as compiled by Clarke (1981) and shown in the inset diagram.

compositional differences were noted in terms of major-element chemistry (Fig. 8). However, a fairly large range in the alkali ratio was found; the muscovite that mantles garnet tends to have the lowest $\text{Na}/(\text{Na} + \text{Ca} + \text{K})$ values (analyses 45 and 8 in Table 5). In the same diagram, the data are compared to Clarke's (1981) field for "primary" muscovite in peraluminous granites. The muscovite in this study is notably depleted in Fe + Mg. The data are also plotted in terms of the cationic proportions of Mg-Ti-Na (Fig. 9), a diagram used by Miller *et al.* (1981) to distinguish between primary and secondary muscovite in granites. Although relatively depleted in Ti compared to the field defined for primary muscovite, the muscovite analyzed in this study is anomalously enriched in the paragonitic (Na) component compared to both the primary and secondary muscovite compositions of Miller *et al.* (1981). This relative enrichment is due to the anomalously low absolute abundances of Ti and Mg compared to the examples studied by those authors. For example, according to their calculations, most examples of plutonic muscovite have 0.2 to 0.5 Fe + Mg cations per formula unit (11 oxygen atoms). This compares with 0.07 to 0.16 for the muscovite in this study.

Garnet was analyzed from the three granitic rocks (representative core and rim compositions are in Table 6), with the data plotted in terms of their major end-member components (Fig. 10) and wt. % CaO and MnO versus FeO (Fig. 11). In these diagrams

two populations are distinguished, one for garnet from the microgranite, and a second for garnet from the monzogranite and dyke-rock.

Garnet from the microgranite (NS-48-1,2,3) varies in composition mainly with respect to its almandine-spessartine components ($\text{Alm}_{71} \text{Spess}_{27}$ to $\text{Alm}_{82} \text{Spess}_{18}$), pyrope being fairly constant at 2-3 mol. %. This variation is correlated with changes in composition from core to rim; five of the six grains analyzed have normal zoning profiles (*i.e.*, a Mn-rich core), as indicated in Figure 11 and Table 6. The sixth grain has an irregular zoning profile. Other chemical characteristics of garnet includes low Ca (constant between 0.1 and 0.2 wt. % CaO), and negligible contents of Na, Ti and Cr.

Garnet in the monzogranite and dyke-rock forms a separate field in the chemical plots, reflecting a relative enrichment in Mg and Ca, although it is also possible to distinguish two subgroups using these data. In general, garnet compositions range from $\text{Alm}_{68} \text{Spess}_{23} \text{Py}_8$ to $\text{Alm}_{76} \text{Spess}_{16} \text{Py}_6$ (Fig. 10) with between 0.25 and 0.5 wt. % CaO, 7.8 to 10.5 wt. % MnO, and 30.0 to 33.05 wt. % FeO. When considered separately, the garnet in the dyke-rock (NS-46-1) intergrown with quartz lacks zoning and is relatively enriched in Ca and Mn, and depleted in Fe compared to garnet in the monzogranite (NS-46-2) only a few cm away. In contrast, the garnet of the monzogranite is zoned from core to rim, with the higher Mn contents generally along the margin,

TABLE 6. REPRESENTATIVE COMPOSITIONS OF GARNET

ANALYSIS NUMBER	70	76	113R	114C	119C	42R	62C	61R	96C	95R	5C	3R
SiO ₂	36.08	37.28	37.79	37.48	36.68	35.56	35.69	36.14	36.97	37.05	35.75	35.90
TiO ₂	0.08	0.09	0.05	0.11	0.14	0.04	0.09	0.04	0.20	0.04	0.07	ND
Al ₂ O ₃	20.07	20.99	20.64	21.20	20.95	20.86	20.79	20.46	20.99	20.77	21.09	20.80
FeO	30.21	30.88	33.05	32.60	31.61	31.55	32.55	34.78	31.10	34.17	33.03	35.38
MnO	10.07	9.73	7.73	8.49	9.98	9.31	10.83	7.87	11.38	7.38	10.02	7.24
MgO	1.64	1.59	1.25	1.29	1.34	1.86	2.36	2.41	0.30	0.53	0.36	0.35
CaO	0.35	0.34	0.25	0.30	0.35	0.30	0.16	0.19	0.16	0.16	0.10	0.15
Na ₂ O	0.04	0.04	0.02	0.02	0.01	ND	0.04	ND	ND	ND	0.04	0.01
Cr ₂ O ₃	ND	ND	0.06	0.02	0.04	0.08	ND	ND	0.01	0.02	ND	0.05
Total	98.56	100.94	100.89	101.51	101.10	99.56	100.51	99.88	101.12	100.12	100.45	99.88
NUMBER OF CATIONS ON THE BASIS OF 12 OXYGEN												
Si	2.996	3.010	3.049	3.010	2.974	2.931	2.943	2.986	3.003	3.032	2.942	2.966
Al ^{iv}	0.004	0.000	0.000	0.000	0.026	0.069	0.057	0.014	0.000	0.000	0.058	0.034
Al ^{vi}	1.961	1.998	1.962	2.006	1.974	1.955	1.964	1.990	2.009	2.003	1.988	1.991
Ti	0.004	0.004	0.004	0.004	0.007	0.002	0.004	0.000	0.012	0.000	0.002	0.000
Fe ²⁺	2.099	2.085	2.230	2.189	2.143	2.174	2.244	2.327	2.112	2.337	2.273	2.445
Mg	0.707	0.664	0.528	0.577	0.685	0.648	0.755	0.613	0.782	0.511	0.698	0.504
Mn	0.202	0.189	0.149	0.153	0.162	0.227	0.043	0.056	0.036	0.062	0.043	0.041
Cr	0.000	0.000	0.002	0.000	0.002	0.004	0.000	0.012	0.000	0.000	0.000	0.002
Na	0.004	0.004	0.002	0.002	0.000	0.000	0.004	0.002	0.000	0.000	0.004	0.000
Ca	0.029	0.028	0.021	0.023	0.028	0.024	0.012	0.012	0.012	0.012	0.007	0.012
END MEMBER GARNET IN MOLECULAR PER CENT												
Spss	23.2	22.4	18.0	19.6	22.7	21.0	24.7	18.2	26.6	17.5	23.1	16.8
Alm	69.1	70.3	76.1	74.4	72.1	70.7	73.5	79.7	71.8	80.0	75.2	81.4
Py	6.7	6.4	5.1	5.2	4.9	7.4	1.4	1.6	1.2	2.1	1.4	1.4
Grs &	0.9	0.9	0.7	0.8	0.9	0.8	0.4	0.5	0.4	0.4	0.3	0.4
Adr												

Analyses are from the following samples:

NS-46-1 : 70,76

NS-46-2 : 113,114,119,42

ND = not detected

NS-48-1 : 62,61

NS-48-2 : 96,95

C = core

R = rim

opposite to that noted in garnet from the microgranite.

With reference to the fields outlined by Clarke (1981) and Miller & Stoddard (1981) for plutonic garnet (Fig. 10), these garnet compositions conform to

those considered indicative of magmatic conditions. Compared to previously published compositions of "magmatic garnet" in the SMB and MB, these samples are intermediate in composition between MacDonald's (1982) very spessartine-rich (28-43 mol.%)

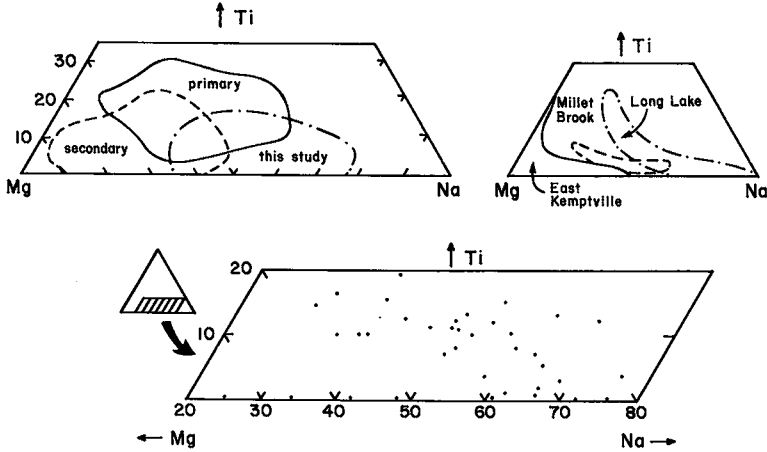


FIG. 9. Compositions of muscovite in the BIPI complex plotted in the ternary diagram Ti-Mg-Na. The fields for primary and secondary muscovite are from Miller *et al.* (1981), and data for the East Kemptville, Long Lake and Millet Brook areas are from Chatterjee & Strong (1985).

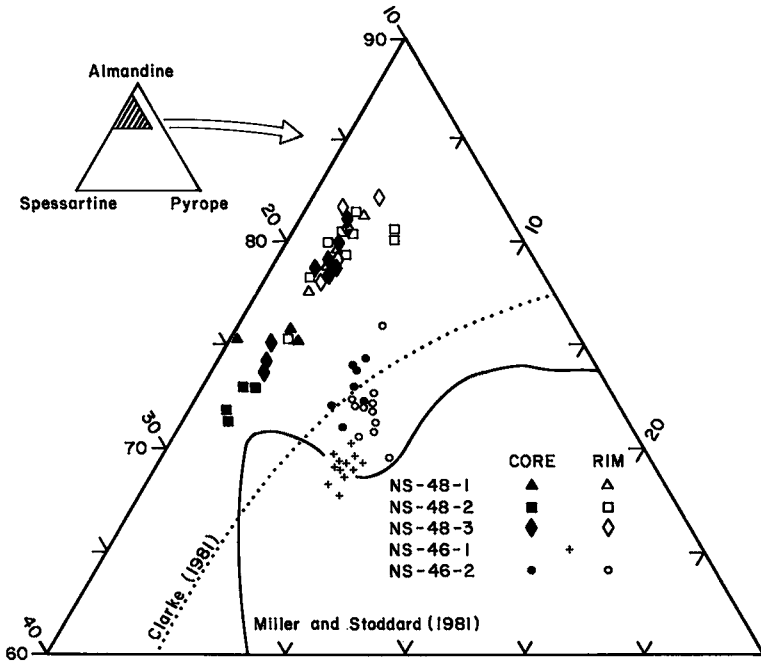


FIG. 10. Compositions of garnet in the BIPI complex plotted in terms of end-member components Almandine-Spessartine-Pyrope. The compositional fields for garnets of magmatic origin are after Clarke (1981) and Miller & Stoddard (1981). For sample NS-46-1 there is no compositional difference between analysis for the margin and core areas of garnet intergrown with the quartz.

garnet found in aplites, and that which occurs in monzogranites and leucogranites and was analyzed by Allan & Clarke (1981) (on average 6.27 and 6.91 wt. % MnO, respectively).

DISCUSSION

Previous discussions concerning the origin of garnet in plutonic rocks of granitic composition have been presented by Miller & Stoddard (1981) and Clarke (1981); the experimental work of Green (1977) and Clemens & Wall (1981) is relevant, as well as the topological examination of the granite system by Abbott & Clarke (1979). In all of these papers the role of Mn is emphasized, its effect being to stabilize garnet to lower pressures and temperatures because Mn is preferentially concentrated in garnet relative to the other silicate minerals. Suggested origins for garnet based primarily on textural evidence, excluding the cases of texturally obvious xenocrystic phases, include the following: (i) the biotite + liquid \rightarrow garnet + muscovite reaction of Miller & Stoddard (1981) resulting from a relative increase in the Mn content of the melt due to magmatic differentiation [may also include liquid-state diffusion processes (Hildreth 1979)]. (ii) The liquid \rightarrow biotite + garnet or liquid + biotite \rightarrow garnet reactions of

Allan & Clarke (1981) proposed for garnet of the SMB.

Another criterion often discussed in determining the origin of garnet is the type of zoning observed. For example, since the advent of electron-microprobe analysis, it has been possible to determine zoning profiles in garnet (*e.g.*, Hollister 1966). As a result of studies of occurrences of metamorphic garnet, it is generally considered that normal zoning profiles reflect prograde metamorphic conditions, and reverse profiles reflect retrograde conditions (*e.g.*, Anderson & Olimpio 1977, Woodsworth 1977). By analogy, it has been assumed that reverse zoning, reflecting falling temperatures, should be characteristic of magmatic garnet (*e.g.*, Allan & Clarke 1981), although normal zoning is also found in garnet considered to be of magmatic origin (MacDonald 1979, 1982, Anderson & Rowley 1981). Thus, it seems that zoning profiles in garnet should not be considered diagnostic of any particular mode of origin.

From the above discussion, the textural and chemical features of the phases coexisting with garnet seem to be of critical importance in determining its origin. Therefore, we emphasize the following textural and chemical features present in the garnet-bearing granites of the BIPI complex which must be considered before discussing the origin of the garnet.

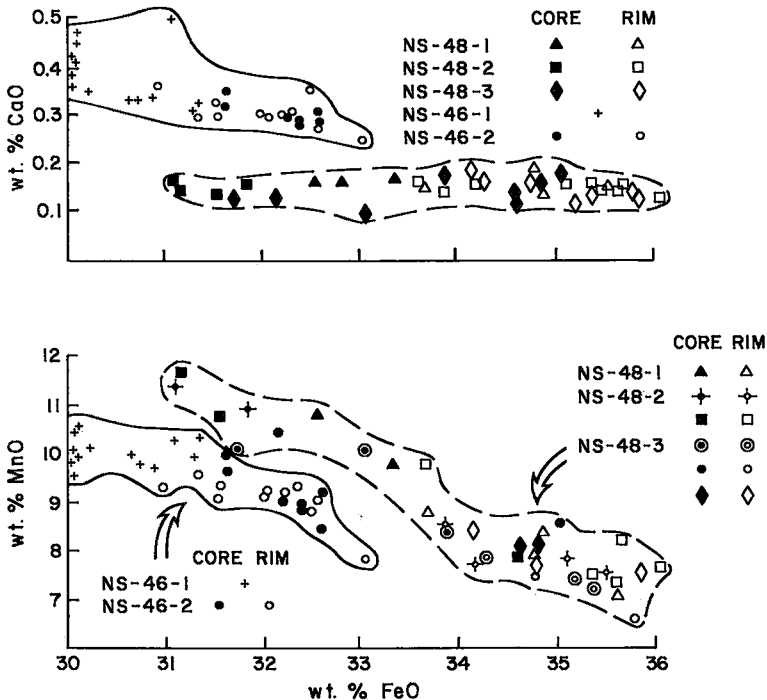


FIG. 11. Compositions of garnet in the BIPI complex plotted as wt.% CaO and MnO versus wt.% FeO.

Textural evidence and distribution of garnet

The granitic rocks of the BIPI complex have undergone considerable postmagmatic textural modification. For example, we have discussed the different textural varieties of muscovite, quartz, alkali feldspar and garnet; in many cases processes other than those of magmatic origin are considered responsible (e.g., muscovite mantling garnet). Corey (1987) has demonstrated that several distinct episodes of hydrothermal alteration within the BIPI complex have resulted in a variety of mineral assemblages, most of which post-date garnet formation. However, important to this discussion is the spatial and temporal relationships of garnet.

Garnet is pervasively developed, but some occurrences are most important in terms of deciphering its genesis. We emphasize the presence of garnet concentrated along intrusive contacts and fractures and occurring within pegmatites. Garnet may be concentrated up to 30–50 vol. % along contact zones. These extreme cases occur most frequently where dykes or the microgranite phase cut earlier monzogranite. Important also is the heterogeneous distribution of garnet, notably in the microgranite where there is a strong antipathetic relationship with biotite. Garnet-rich areas lack biotite, and many show enrichment in albite or alkali feldspar compared to biotite-bearing parts of the rock. Thus, there is a tendency for garnet to be developed along certain structural features and with some late-stage rocks (e.g., pegmatites).

Garnet textures, as previously discussed, correspond to two distinct types, *viz.* small euhedral grains, and larger anhedral clots with quartz inclusions. Both varieties occur in the microgranite and dyke-rocks, but only the euhedral variety is observed in the monzogranite. The texture of the garnet-quartz clots is anomalous in being considerably coarser than the rest of the rock. Had the garnet crystallized at the same time as the rest of the mineral phases, all might be expected to be of similar size.

At least two origins may be postulated for the garnet-quartz intergrowths: (i) cocrystallization and (ii) replacement. In the first, the texture is somewhat analogous to the graphic intergrowth of quartz and feldspar commonly observed in granitic rocks. The presence of metasomatic zones about these garnet-quartz clots, the absence of biotite in such areas, and the generally much coarser texture for the clots than the rest of the rock indicate a probable postmagmatic age for their formation. Similarly, one might also expect to find quartz and feldspar arranged in graphic intergrowths in the same rocks if this texture formed during a period of rapid, late-magmatic crystallization. Thus, if this texture represents cocrystallization, then we favor at least a late-stage, postmagmatic time of formation.

In the second scenario, the intergrowth may have resulted from replacement of the primary granite mineralogy by garnet. In this case only quartz remained, the other constituents having either been consumed during the garnet-forming reaction or dissolved and removed during the process. This type of texture is not unlike that seen in metamorphic rocks where porphyroblastic, poikilitic-rich garnet or cordierite is developed. As in the first case, a late-stage, postmagmatic origin is suggested.

Although we favor a postmagmatic or subsolidus origin for the garnet described here, we do note that a very similar occurrence of garnet in late-Variscan granites of the Bavarian Forest region was interpreted by Propach & Gillissen (1984: see their Fig. 2) as being magmatic. These authors favored a reaction between early biotite and cordierite to form garnet with the reaction having consumed all the available biotite. It should be noted, however, that the texture of the garnet-quartz intergrowth is not discussed and, despite the high spessartine component (*ca.* 15 mol.%) of the garnet, the whole-rock chemistry is characterized by anomalously low Mn/(Mn + Fe) ratios.

The timing of garnet development is provided from textural relationships. Garnet clearly overgrew earlier magmatic phases, was in turn mantled by muscovite, and elsewhere in the BIPI complex was overprinted by later stage alteration (Corey 1987 and in prep.). As the above textural evidence is interpreted to reflect a postmagmatic origin, this additional constraint suggests a very early time of formation in relation to the other alteration events.

The development of sillimanite and andalusite, in zones of hyperaluminous alteration (Corey 1987) that post-date garnet growth, permits an estimate of the temperatures which attended the alteration event. Essential to this argument, however, is that the fluid causing these alteration zones is a single fluid that causes progressive alteration but changes chemically during this event. If this assumption is correct, then a temperature of at least 520°C (at *P* = 3.9 kbars; Robie & Hemingway 1984) is inferred. As the level of emplacement is considered to be less than *ca.* 12 km, then higher temperatures would be inferred. However, sillimanite occurs as the fibrolitic variety after biotite, and thus temperature estimates must be viewed cautiously in light of the recent investigations of the metastable behavior of this phase (Kerrick 1987). This temperature is similar to the maximum temperature inferred from the two-feldspar geothermometry for the microgranite samples (see above) and is consistent with the presence of orthoclase as the dominant alkali feldspar polymorph (*cf.* Bambauer & Bernotat 1982).

Chemical evidence

Mineral chemistry of the major silicate phases

present indicates marked deviations from magmatic compositions. The plagioclase in the microgranite and dyke-rock are invariably albitic (*i.e.*, An_{0-7}), well removed from even the low-temperature end of the ternary for feldspar equilibria (Parsons & Brown 1984). Also, plagioclase (An_{17-11}) of presumably magmatic origin occurs with later albite (An_{2-7}) in the monzogranite, indicating apparent disequilibrium due to postmagmatic processes.

The composition of the white-mica phases deviate markedly from the fields outlined by Clarke (1981) and Miller *et al.* (1981) for primary muscovite occurring in peraluminous granites. Instead, the compositions are more similar to secondary white mica found associated with lithophile-element mineralization elsewhere in the SMB. In Figures 7 and 8 we compare the BIPI mica analyses to compositions of secondary mica obtained by Chatterjee & Strong (1985) for some of these mineralized greisens. Our analyses show a much more restricted range in the Si-Al-(Fe + Mg + Mn) triangular plot compared to their data, the reason for this not being readily apparent. However, an increasing celadonitic component in muscovite is considered to expand its stability field to higher temperature (Anderson & Rowley 1981); therefore, the chemical differences indicated may reflect in part a variety of temperatures attending the alteration events. The restricted range in the BIPI muscovite compositions might be interpreted to reflect a short temperature interval during which the micas either crystallized or re-equilibrated. It is also suggested that the high paragonitic component of the muscovite is due to a high activity of Na in the fluids during alteration.

Biotite compositions, albeit obtained only for the microgranite, are characterized by high Fe/(Fe + Mg) values and low absolute abundances of Ti. As noted above, the biotite data fall outside of Clarke's (1981) field for compositions typical of peraluminous granites and the Fe/(Fe + Mg) values are higher than generally reported for primary biotite in the SMB. The low absolute Ti contents maybe due to later equilibration with a fluid phase that also may have modified the Fe/(Fe + Mg) ratios, which are dependent on fO_2 . Taner *et al.* (1986) and Le Bel (1979) also have noted low absolute Ti contents of biotite in alteration zones and have concluded that it reflects low temperatures of the hydrothermal fluids, presumably relative to magmatic conditions. Thus, the chemistry of the biotite may not represent primary, magmatic compositions.

The garnet grains have been shown to define both normal (NS-48-1,2,3) and reverse (NS-46-2) zoning profiles, or no apparent zonation at all (NS-46-1). Although the compositions correspond broadly to the field defined by Miller & Stoddard (1981) for magmatic garnet, the compositions of garnet from two of the samples fall outside of Clarke's (1981)

field for magmatic garnet. In addition, the garnet compositions define two populations, which is consistent with there being different host rocks.

That all of the garnet owes its existence to the same general process is assumed, based on the broadly similar petrographic and field relationships. This being the case, then why such a radical difference in chemistry between the two populations? The most viable solution lies in the bulk composition of the host-rock lithologies. The garnet within the monzogranite and dyke-rock represents an environment enriched in Ca and Mg relative to the microgranite, precisely the elements garnet is enhanced in.

Origin of the garnet

From the foregoing discussion of the petrographic and chemical features of the garnet and associated silicate minerals, we suggest that garnet formation occurred as a result of postmagmatic phenomena. The evidence presented indicates that most of the silicate-mineral chemistry is not of primary magmatic nature, and the textural relationships of the phases also indicate late-stage re-equilibration or growth (or both). The ubiquitous occurrence of garnet throughout the 18–20 km² area of the BIPI complex indicates that the nature of the processes which caused the re-equilibration of the host rocks into their present assemblage was pervasive. Considering the lack of petrographic evidence to support a magmatic origin *via* the reaction mechanisms of Miller & Stoddard (1981) and Allan & Clarke (1981), and the different chemistries of the garnet compared to potential garnet xenocrysts from a Meguma Group contaminant (Jamieson 1974), a metasomatic origin seems most reasonable.

Based on the textural and chemical features of the garnet and associated phases, the following mechanism is suggested. Firstly, the antipathetic relationship between garnet and biotite is consistent with the latter being a contributor of some of the ferromagnesian components. Similarly, the involvement of plagioclase is suggested by the presence of calcium within the garnet. We have estimated the approximate gains and losses that may have occurred during transformation of an aliquot of "pristine" biotite monzogranite to a similar volume of rock consisting of quartz and garnet using representative mineral compositions. As shown in Figure 12, there is a net % gain of Fe, Mn, Al and Mg, and a net % loss of Si, Na, K and Ca. It can be easily imagined that the latter elements may have contributed to the development of alkali metasomatism, greisenization and even formation of apatite-rich zones within the BIPI complex (Corey 1986, 1987), but the source of the elements involved in the transformation is more speculative. Three potential sources are considered, *viz.* late-stage fluids of dominantly unmodified mag-

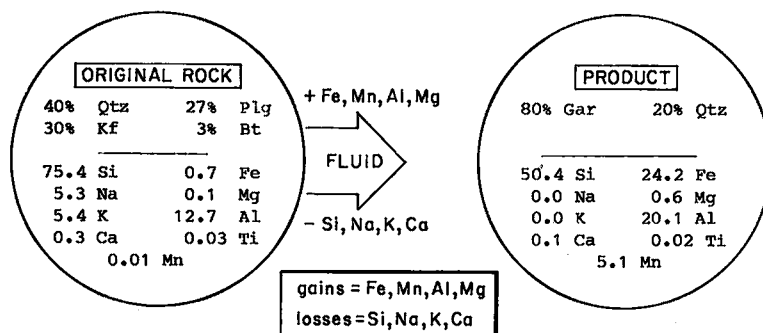


FIG. 12. Diagrammatic representation of alteration of original biotite-bearing microgranite lithology to garnet-quartz segregation due to fluid interaction. Calculations done for 100 grams of reactants and products.

matic origin, and fluids which are in part magmatic but which have an extraneous component derived from either the granodiorite phase of the BIPI complex or from metasedimentary rocks of the Meguma Group.

In the first case, fluids derived from fractionation of the most evolved phases of the BIPI complex represent a likely source. Such fluids are considered to be responsible for extensive metasomatism within granitic rocks (e.g., Pollard 1983, Pollard & Taylor 1986, Stone & Exley 1986). Although late-stage magmatic fluids may contain quantities of Fe, Mg and Mn in the form of chloride complexes (Burnham 1979), the alteration generally associated with such juvenile fluids is characteristically dominated by alkali-rich phases. Although some of the elemental components of concern can be provided by altering the mafic constituents (e.g., biotite) of the host granite, there is a deficiency of these elements in the rocks of interest (see above).

In the second case, the granodiorite is potentially an excellent reservoir for the elements of interest. However, if fluids did interact with this unit, they did not alter it at the present level of exposure. In fact, it is perplexing why the granodiorite is so fresh relative to the other granitoid phases.

The final source is represented by the metasedimentary rocks of the Meguma Group. That late-stage granites of the SMB have been contaminated to a certain degree by the metasedimentary rocks of the Meguma Group *via* fluid interaction is supported by both sulfur (Kubilius & Ohmoto 1982) and oxygen (Kontak & Kerrich, in prep.) isotopic studies. Thus, we suggest that at some late-magmatic or early postmagmatic stage extraneous components (i.e., Fe, Mn, Al, Mg) were introduced *via* some mechanism of fluid interaction with Meguma Group lithologies.

CONCLUSIONS

The widespread development of spessartine-rich almandine garnet in a late-stage, polyphase intrusion of the SMB is described and a postmagmatic, metasomatic origin is suggested. The formation of this phase is considered to have occurred at temperatures in excess of 500–550°C and represents the first stage of several distinct periods of superimposed alteration types (Corey 1987 and in prep.). The formation of garnet-quartz clots requires the local gain of Fe, Mg, Al and Mn in excess of what can be provided by a similar volume of unaltered host rock. Thus it is proposed that some of this gain was derived from the surrounding Meguma Group metasedimentary rocks through fluid interaction.

The silicate mineralogy of the host granitoids reflects the interaction of the granite with hydrothermal solutions such that very little remains of what can be referred to as magmatic. Manning & Exley (1984) and Stone & Exley (1986) have described similar postmagmatic processes to account for the origin of the lithium-mica granites of the St. Austell area, southwest England, and several authors have documented the effects of metasomatism in the mineralized anorogenic granites of Nigeria (Martin & Bowden 1981, Ike *et al.* 1985, Kinnaird *et al.* 1985). Thus, occurrence of metasomatism in the BIPI complex is not unique with respect to granitoid petrology, but the presence of metasomatic garnet is unusual and again warrants caution concerning the interpretation of what is and is not of primary magmatic origin in granitoid rocks.

ACKNOWLEDGEMENTS

The Nova Scotia Department of Mines and Energy (Mineral Development Division) is acknowledged for supporting the field work for this study, and for

providing technical facilities to prepare the manuscript and illustrations. The electron-microprobe analyses were obtained at Memorial University of Newfoundland with the capable assistance of G. Veinott and H. Longridge. D.K. is grateful to D.F. Strong for providing post-doctoral financial support (from NSERC Operating Grant No. A7975), and for many hours of enlightened discussion on the various problems of granite petrogenesis. Discussions with M.A. MacDonald, L.J. Ham, R. Horne, G.A. O'Reilly and A.K. Chatterjee contributed to our better understanding of the general problems of granite petrogenesis, especially the SMB, and are gratefully acknowledged. Critical reading of the manuscript by several of our colleagues resulted in substantial improvements; however, the authors bear full responsibility for the opinions presented. The comments offered by two anonymous reviewers and the editors helped to substantially improve the manuscript and clarify several technical points.

REFERENCES

- ABBOTT, R.N. & CLARKE, D.B. (1979): Hypothetical liquidus relationships in the subsystem Al_2O_3 -FeO-MgO projected from quartz, alkali feldspar and plagioclase for $a(H_2O) \leq 1$. *Can. Mineral.* **17**, 549-560.
- ALLAN, B.D. & CLARKE, D.B. (1981): Occurrence and origin of garnets in the South Mountain Batholith, Nova Scotia. *Can. Mineral.* **19**, 19-24.
- ANDERSON, D.A. & OLIMPIO, J.C. (1977): Progressive homogenization of metamorphic garnets, South Morar, Scotland: evidence for volume diffusion. *Can. Mineral.* **15**, 205-216.
- ANDERSON, J.L. & ROWLEY, M.C. (1981): Synkinematic intrusion of peraluminous and associated metaluminous granitic magmas, Whipple Mountains, California. *Can. Mineral.* **19**, 83-102.
- BAMBAUER, H.V. & BERNOTAT, W.H. (1982): The microcline/sandine transformation isograd in metamorphic regions I. Composition and structural state of alkali feldspars from granitoid rocks of two N-S traverses across the Aar Massif and Gotthard "Massif", Swiss Alps. *Schweiz. Mineral. Petrogr. Mitt.* **62**, 185-230.
- BENCE, A.E. & ALBEE, A. (1968): Empirical correction factors for the electron microanalysis of silicates and oxides. *J. Geol.* **76**, 382-403.
- BURNHAM, C.W. (1979): Magmas and hydrothermal fluids. In *Geochemistry of Hydrothermal Ore Deposits* (H.L. Barnes, ed.). John Wiley & Sons, New York, 71-136.
- ČERNÝ, P., SMITH, J.V., MASON, R.A. & DELANEY, J.S. (1984): Geochemistry and petrology of feldspar crystallization in the Vezna pegmatite, Czechoslovakia. *Can. Mineral.* **22**, 631-651.
- CHATTERJEE, A.K. & STRONG, D.F. (1985): A review of some chemical and mineralogical characteristics of granitoid rocks hosting Sn, W, U, Mo deposits in Newfoundland and Nova Scotia. In *High Heat Production Granites, Hydrothermal Circulation and Ore Genesis*. Inst. Min. & Metall. Publ., London, England.
- _____, _____ & CLARKE, D.B. (1985): Petrology of the polymetallic quartz-topaz greisen at East Kempville. In *Guide to the Granites and Mineral Deposits of Southwestern Nova Scotia* (A.K. Chatterjee & D.B. Clarke, eds.). Nova Scotia Dep. Mines & Energy, Paper 85-3.
- CLARKE, D.B. (1981): The mineralogy of peraluminous granites: a review. *Can. Mineral.* **19**, 3-19.
- _____, _____ & CHATTERJEE, A.K. (1985): Physical and chemical processes in the South Mountain Batholith. In *Granite-Related Mineral Deposits: Geology, Petrogenesis and Tectonic Setting* (R.P. Taylor & D.F. Strong, eds.). Can. Inst. Mining Metall. Conf., Halifax, N.S.
- _____, _____ & HALLIDAY, A.N. (1980): Strontium isotope geology of the South Mountain Batholith, Nova Scotia. *Geochim. Cosmochim. Acta* **44**, 1045-1058.
- _____, _____ & MUECKE, G.K. (1985): Review of the petrochemistry and origin of the South Mountain Batholith and associated plutons, Nova Scotia, Canada. In *High Heat Production Granites, Hydrothermal Circulation and Ore Genesis*. Inst. Mining Metall. Publ., London, England.
- CLEMENS, J.D. & WALL, V.J. (1981): Origin and crystallization of some peraluminous (S-type) granitic magmas. *Can. Mineral.* **19**, 111-132.
- COREY, M.C. (1986): Bedrock geology of the South Mountain Batholith: NTS map sheet 11D/13. *Nova Scotia Dep. Mines Energy Rep. Activities, Rep.* **86-1**, 137-147.
- _____, _____ (1987): Hydrothermal alteration and associated mineralization within a polyphase intrusive complex from the South Mountain Batholith. *Atlantic Geosciences Soc. Spring Meeting, Program Abstr.*
- FOSTER, M.D. (1960): Interpretation of the composition of trioctahedral micas. *U.S. Geol. Surv. Prof. Paper* **354-B**, 11-42.
- GREEN, T.H. (1977): Garnet in silicic liquids and its possible use as a P-T indicator. *Contrib. Mineral. Petrology* **15**, 59-67.
- HAMER, R.D. & MOYES, A.B. (1982): Composition and origin of garnet from the Antarctic Peninsula Vol-

- canic Group of Trinity Peninsula. *J. Geol. Soc. Lond.* **139**, 713-720.
- HILDRETH, W. (1979): The Bishop Tuff: evidence for the origin of compositional zonation in silicic magma chambers. *Geol. Soc. Amer. Spec. Paper* **180**, 43-75.
- HOLLISTER, L.S. (1966): Garnet zoning: an interpretation based on the Rayleigh fractionation model. *Science* **154**, 1647-1651.
- IKE, E., BOWDEN, P. & MARTIN, R.F. (1985): Amphibole in the porphyries of the Tibchi anorogenic ring-complex, Nigeria: product of deuteritic adjustments. *Can. Mineral.* **23**, 447-456.
- JAMIESON, R.A. (1974): *The Contact of the South Mountain Batholith Near Mt. Uniacke, Nova Scotia*. B.Sc. thesis, Dalhousie Univ., Halifax, N.S.
- KEPPIE, J.D. (1979): Geological map of the province of Nova Scotia, 1:500,000 scale. *Nova Scotia Dep. Mines Energy Publ.*
- KERRICK, D.M. (1987): Fibrolite in contact aureoles of Donegal, Ireland. *Amer. Mineral.* **72**, 240-254.
- KINNAIRD, J.A., BATCHELOR, R.A., WHITLEY, J.E. & MACKENZIE, A.B. (1985): Geochemistry, mineralization and hydrothermal alteration of Nigerian high heat producing granites. In *High Heat Production Granites, Hydrothermal Circulation and Ore Genesis*. Inst. Mining Metall. Publ., London, England.
- KUBILIUS, W.P. & OHMOTO, H. (1982): Sulphur isotope study of peraluminous granitoids and associated metasediments, southern Nova Scotia, Canada. *Geol. Assoc. Amer., Abstr. Program* **82**, 536.
- LE BEL, L. (1979): Micas magmatiques et hydrothermaux dans l'environnement du porphyre cuprifère de Cerro Verde - Santa Rosa, Pérou. *Bull. Minéral.* **102**, 35-41.
- MACDONALD, M.A. (1979): The mineralogy and petrology of garnet-bearing rocks from southern Nova Scotia. Unpubl. Report, Dalhousie Univ., Halifax, N.S.
- _____ (1982): *The Mineralogy, Petrology and Geochemistry of the Musquodoboit Batholith*. M.Sc. thesis, Dalhousie Univ., Halifax, N.S.
- MANNING, D.A.C. & EXLEY, C.S. (1984): The origins of late-stage rocks in the St. Austell granite - a re-interpretation. *J. Geol. Soc. Lond.* **141**, 581-591.
- MARTIN, R.F. & BOWDEN, P. (1981): Peraluminous granites produced by rock-fluid interaction in the Ririwai nonorogenic ring-complex, Nigeria: mineralogical evidence. *Can. Mineral.* **19**, 65-82.
- McKENZIE, C.B. & CLARKE, D.B. (1975): Petrology of the South Mountain Batholith, Nova Scotia. *Can. J. Earth Sci.* **12**, 1209-1218.
- MILLER, C.F. & STODDARD, E.F. (1981): The role of manganese in the paragenesis of magmatic garnet: an example from the Old Woman-Piute Range, California. *J. Geol.* **89**, 233-246.
- _____, _____, BRADFISH, L.J. & DOLLASE, W.A. (1981): Composition of plutonic muscovite: genetic implications. *Can. Mineral.* **19**, 25-35.
- PARSONS, I. & BROWN, W.L. (1984): Feldspars and the thermal history of igneous rocks. In *Feldspars and Feldspathoids: Structures, Properties and Occurrences* (W.L. Brown, ed.). NATO ASI Series, D. Reidel Publ. Co., Dordrecht, Holland.
- PATTISON, D.R.M., CARMICHAEL, D.M. & ST-ONGE, M.R. (1982): Geothermometry and geobarometry applied to Early Proterozoic "S-type" granitoid plutons, Wopmay Orogeny, Northwest Territories, Canada. *Contr. Mineral. Petrology* **79**, 394-404.
- POLLARD, P.J. (1983): Magmatic and postmagmatic processes in the formation of rocks associated with rare-element deposits. *Trans. Inst. Mining Metall.* **92**, B1-B9.
- _____ & TAYLOR, R.G. (1986): Progressive evolution of alteration and tin mineralization: controls by interstitial permeability and fracture-related tapping of magmatic fluid reservoirs in tin granites. *Econ. Geol.* **81**, 1795-1800.
- PROPACH, G. & GILLESSEN, B. (1984): Petrology of garnet-, spinel-, and sillimanite-bearing granites from the Bavarian Forest, West Germany. *Tschermaks Mineral. Petr. Mitt.* **33**, 67-75.
- REYNOLDS, P.H., ZENTILLI, M. & MUECKE, G.K. (1981): K-Ar and ⁴⁰Ar/³⁹Ar geochronology of granitoid rocks from southern Nova Scotia: its bearing on the geological evolution of the Meguma Zone of the Appalachians. *Can. J. Earth Sci.* **18**, 386-394.
- ROBIE, R.A. & HEMINGWAY, B.S. (1984): Entropies of kyanite, andalusite, and sillimanite: Additional constraints on the pressure and temperature of the Al₂SiO₅ triple point. *Amer. Mineral.* **69**, 298-306.
- RYAN, A.B. (1984): Regional geology of the central part of the central mineral belt, Labrador, Newfoundland. *Newfoundland Dep. Mines Energy, Mineral Development Div., Mem.* **3**.
- STONE, M. & EXLEY, C.S. (1986): High heat production granites of southwest England and their associated mineralization: a review. *Trans. Inst. Mining Metall. Sect. B*, **95**, B25-B36.
- STORMER, J.C., JR. (1975): A practical two-feldspar geothermometer. *Amer. Mineral.* **60**, 667-674.

- STRECKEISEN, A.L. (1976): To each plutonic rock its proper name. *Earth Science Review* 12, 1-33.
- TANER, M.F., TRUDEL, P. & PERRAULT, G. (1986): Géochimie de la biotite associée à certains gisements d'or de Val D'Or, Malartic et Chibougamau, Québec. *Can. Mineral.* 24, 761-774.
- WOODSWORTH, G.J. (1977): Homogenization of zoned garnets from pelitic schists. *Can. Mineral.* 15, 230-242.
- WHITNEY, J.A. & STORMER, J.C., JR. (1977): The distribution of $\text{NaAlSi}_3\text{O}_8$ between coexisting microcline and plagioclase and its effect on geothermometric calculations. *Amer. Mineral.* 62, 687-691.

Received April 16, 1986; revised manuscript accepted May 22, 1987.